以 3,5-二溴苯甲酸及吡啶构筑的一维镉(II)和锰(II)配位聚合物的合成、晶体结构、荧光及磁性质

高竹青*,1　李红晋 1　顾金忠*,2

(1 太原科技大学化学与生物工程学院,太原　030021)

(2 甘肃省有色金属化学与资源利用重点实验室,兰州大学化学化工学院,兰州　730000)

摘要：通过水热方法,以 3,5-二溴苯甲酸(3,5-HBr₂BC)和吡啶(py)分别与 Cd(NO₃)₂·4H₂O 和 MnSO₄·2H₂O 反应,合成了 2 个具有同质异心结构的一维链状配位聚合物[M₃(3,5-Br₂BC)₆(py)₂]ₙ(M=Cd,**1**;Mn,**2**),并对其结构、荧光和磁性质进行了研究。结构分析结果表明 2 个化合物属于三斜晶系,$P\overline{1}$ 空间群。这些配合物具有一维链状结构,而且这些一维链状结构通过 Br···Br 卤键和 C-H···Br 氢键作用进一步形成了三维超分子框架。配合物 **1** 在室温下能分别发出很强的绿色荧光,配合物 **2** 中相邻锰离子间存在反铁磁相互作用。

关键词：配位聚合物；卤键；3,5-二溴苯甲酸；荧光；磁性

Synthesis, Crystal Structures, Luminescent and Magnetic Properties of 1D Cadmium(II) and Manganese Coordination Polymers Constructed from 3,5-Dibromobenzoic Acid and Pyridine

GAO Zhu-Qing*,1　LI Hong-Jin1　GU Jin-Zhong*,2

(1School of Chemical and Biological Engineering, Taiyuan University of Science and Technology, Taiyuan 030021, China)

(2Key Laboratory of Nonferrous Metal Chemistry and Resources Utilization of Gansu Provinc, College of Chemistry and Chemical Engineering, Lanzhou University, Lanzhou 730000, China)

Abstract: Two coordination polymers, namely [M₃(3,5-Br₂BC)₆(py)₂]ₙ (M=Cd, **1**; Mn, **2**), have been constructed hydrothermally using 3,5-HBr₂BC (3,5-HBr₂BC=3,5-dibromobenzoic acid), py (py=pyridine), and the corresponding metal salts. Single-crystal X-ray diffraction analyses revealed that the two complexes are isostructural and crystallize in the triclinic system, space group $P\overline{1}$ The carboxylate groups of 3,5-Br₂BC⁻ ligands bridge alternately neighboring metal ions to form a chain. Adjacent chains are assembled to a 3D supramolecular framework through Br···Br halogen bonding and C-H···Br hydrogen bond. Luminescent and magnetic properties of both compounds have also been studied. CCDC: 990799, **1**; 990800, **2**.

Key words: coordination polymer; halogen bonding; 3,5-dibromobenzoic acid; luminescent properties; magnetic properties

In the last two decades, more and more researchers have paid attention to the metallosupramolecular chemistry owing to the generation of materials with various intriguing structural topologies and their potential applications in the areas of catalysis, gas storage, separation, luminescence, and magnetism[1-10].

The self-assembly of a suprmolecular coordination polymer is the result of a combination of various forces, including not only strong interactions (for example metal-ligand coordination bonds) but also weaker interactions such as hydrogen bonds and π-π stacking interactions [11-13]. Although the latter interactions are relatively weak, they have been recognized to play critical roles in the construction of supramolecular structures. Recently, halogen-related interactions, including halogen bonding as well as related halogen$\cdots$halogen and halogen $\cdots$ π intermolecular interactions have been another attractive interactions in crystal engineering [14-16]. However, the role of halogen bonding effects on assembly of metal-orgnic networks remains largely unexplored and needs more elaborate and systematic research. Attempted assembly of discrete coordination complexes using halogen bonding or halogen$\cdots$halogen interactions into 1D or 2D supramolecular structures has proven its difficulty [17-18]. In order to extend our research in this field, we chose 3,5-dibromobenzoic acid (3,5-HBr$_2$BC) as a functional ligand, which based on the following considerations: (a) 3,5-HBr$_2$BC possesses one carboxyl group for coordination to metal center, and its two Br atoms are potentially capable of taking part in oxygen (or nitrogen) $\cdots$Br halogen bonding and related Br$\cdots$$\pi$ and Br$\cdots$Br interactions; (b) to our knowledge, 3,5-HBr$_2$BC ligand has not been adequately explored in the construction of metal coordination polymers.

Taking into account these factors, we herein report the synthesis, crystal structures, luminescent and magnetic properties of Cd (Ⅱ) and Mn (Ⅱ) coordination polymers constructed from 3,5-Br$_2$BC$^-$ and py ligands.

1 Experimental

1.1 Reagents and physical measurements

All chemicals and solvents were of AR grade and used without further purification. Carbon, hydrogen and nitrogen were determined using an Elementar Vario EL elemental analyzer. IR spectra were recorded using KBr pellets and a Bruker EQUINOX 55 spectrometer. Thermogravimetric analysis (TGA) data were collected on a LINSEIS STA PT1600 thermal analyzer with a heating rate of 10 ℃·min^{-1}. Powder X-ray diffraction patterns (PXRD) were determined with a Rigaku-Dmax 2400 diffractometer using Cu-$K\alpha$ radiation (λ=0.154 060 nm), in which the X-ray tube was operated at 40 kV and 40 mV. Excitation and emission spectra were recorded for the solid samples on an Edinburgh FLS920 fluorescence spectrometer at room temperature. Magnetic susceptibility data were collected in the 2~300 K temperature range with a Quantum Design SQUID Magnetometer MPMS XL-7 with a field of 0.1 T. A correction was made for the diamagnetic contribution prior to data analysis.

1.2 Synthesis of [M$_3$(3,5-Br$_2$BC)$_6$(py)$_2$]$_n$ (M=Cd, 1; Mn, 2)

A mixture of Cd(NO$_3$)$_2$·4H$_2$O (0.046 g, 0.15 mmol), 3,5-HBr$_2$BC (0.083 g, 0.3 mmol), py (0.3 mL), and H$_2$O (10 mL) was stirred at room temperature for 15 min, and then sealed in a 25 mL Teflon-lined stainless steel vessel, and heated at 160 ℃ for 3 d, followed by cooling to room temperature at a rate of 10 ℃·h^{-1}. Colourless block-shaped crystals of **1** were isolated manually, and washed with distilled water. Yield: 65 % (based on Cd). Anal. Calcd. for C$_{52}$H$_{28}$Br$_{12}$Cd$_3$N$_2$O$_{12}$ (%): C 28.80, H 1.30, N 1.29; Found (%): C 28.47, H 1.45, N 1.51. IR (KBr, cm^{-1}): 1 598m, 1 549s, 1 434m, 1 372s, 1 285w, 1 152w, 10 99w, 1 070w, 1 039w, 1 012w, 908w, 869m, 783m, 738m, 697m, 658w, 548w.

Complex **2** was obtained as yellow block-shaped crystals in a manner similar to that used to obtain complex **1**, except using MnSO$_4$·2H$_2$O instead of Cd(NO$_3$)$_2$·4H$_2$O Yield: 70% (based on Mn). Anal. Calcd. for C$_{52}$H$_{28}$Br$_{12}$Mn$_3$N$_2$O$_{12}$ (%): C 31.28, H 1.41, N 1.40. Found (%): C, 31.56; H, 1.17; N, 1.74. IR (KBr, cm^{-1}): 1 603m, 1 550vs, 1 443m, 1 376s, 1 283m, 1 150w, 1 100w, 1 070w, 1040w, 1010w, 908w, 871m, 784m, 739m, 696m, 657w, 552w. The compounds are insoluble in water and common organic solvents, such as methanol, ethanol, acetone, and DMF.

1.3 Structure determinations

Single-crystal data of compounds **1** and **2** were collected at 293 (2) K on a Bruker Smart Apex 1000

CCD diffractometer with Mo $K\alpha$ radiation (λ=0.071 073 nm). A summary of the crystallography data and structure refinement is given in Table 1, and selected bond lengths and angles are listed in Table 2. The structures were solved using direct methods, which yielded the positions of all non-hydrogen atoms. These were refined first isotropically and then anisotropically.

All the hydrogen atoms were placed in calculated positions with fixed isotropic thermal parameters and included in structure factor calculations in the final stage of full-matrix least-squares refinement. All calculations were performed using the SHELXTL-97 system[19].

CCDC: 990799, **1**; 990800, **2**.

Table 1 Crystal data for compounds 1 and 2

Compound	**1**	**2**
Chemical formula	$C_{52}H_{28}Br_{12}Cd_3N_2O_{12}$	$C_{52}H_{28}Br_{12}Mn_3N_2O_{12}$
Molecular weight	2 168.88	1 996.50
Crystal system	Triclinic	Triclinic
Space group	$P\bar{1}$	$P\bar{1}$
a / nm	0.959 35(8)	0.943 58(6)
b / nm	1.107 74(8)	1.118 19(7)
c / nm	1.544 29(12)	1.537 94(15)
α / (°)	71.727(7)	70.948(7)
β / (°)	82.003(7)	82.226(7)
γ / (°)	87.882(6)	88.691(5)
V / nm³	1.543 2(2)	1.519 3(2)
Z	1	1
$F(000)$	1 014	945
Crystal size / mm	0.30×0.28×0.26	0.28×0.26×0.25
θ range for data collection	3.29~25.10	2.94~25.10
Limiting indices	$-10 \leqslant h \leqslant 11, -13 \leqslant k \leqslant 13, -18 \leqslant l \leqslant 18$	$-10 \leqslant h \leqslant 11, -13 \leqslant k \leqslant 11, -18 \leqslant l \leqslant 17$
Reflections collected / unique (R_{int})	9 433 / 5 502 (0.049 1)	9 348 / 5 417 (0.051 6)
D_c / (g·cm⁻³)	2.334	2.182
μ / mm⁻¹	8.851	8.563
Data / restraints / parameters	5 502 / 0 / 368	5 417 / 0 / 368
Goodness-of-fit on F^2	1.011	1.036
Final R indices ($I \geqslant 2\sigma(I)$) R_1, ωR_2	0.051 7, 0.089 9	0.058 0, 0.109 1
R indices (all data) R_1, ωR_2	0.079 4, 0.106 5	0.099 8, 0.137 2
Largest diff. peak and hole / (e·nm⁻³)	961 and −1 129	735 and −850

Table 2 Selected bond distances (nm) and bond angles (°) for compounds 1 and 2

1					
Cd(1)-O(1)	0.230 0(5)	Cd(1)-O(2)	0.250 2(5)	Cd(1)-O(3)	0.248 7(5)
Cd(1)-O(3)A	0.227 8(5)	Cd(1)-O(4)	0.250 5(5)	Cd(1)-O(6)	0.220 7(5)
Cd(1)-N(1)	0.229 5(6)	Cd(2)-O(2)	0.226 6(5)	Cd(2)-O(2)B	0.226 6(5)
Cd(2)-O(4)	0.237 8(5)	Cd(2)-O(4)B	0.237 8(5)	Cd(2)-O(5)	0.218 8(5)
Cd(2)-O(5)B	0.218 8(5)				
O(6)-Cd(1)-O(3)A	85.86(19)	O(6)-Cd(1)-N(1)	171.7(2)	O(3)A-Cd(1)-N(1)	98.1(2)

Continued Table 2

O(6)-Cd(1)-O(1)	88.6(2)	O(3)A-Cd(1)-O(1)	99.07(19)	N(1)-Cd(1)-O(1)	97.9(2)
O(6)-Cd(1)-O(3)	88.29(19)	O(3)A-Cd(1)-O(3)	79.73(18)	N(1)-Cd(1)-O(3)	85.2(2)
O(1)-Cd(1)-O(3)	176.76(17)	O(6)-Cd(1)-O(2)	94.29(18)	O(3)A-Cd(1)-O(2)	153.36(18)
N(1)-Cd(1)-O(2)	85.42(19)	O(1)-Cd(1)-O(2)	54.34(17)	O(3)-Cd(1)-O(2)	126.91(16)
O(6)-Cd(1)-O(4)	86.56(19)	O(3)A-Cd(1)-O(4)	131.15(17)	N(1)-Cd(1)-O(4)	85.30(19)
O(1)-Cd(1)-O(4)	128.89(18)	O(3)-Cd(1)-O(4)	51.85(15)	O(2)-Cd(1)-O(4)	75.34(16)
O(5)B-Cd(2)-O(2)	90.77(19)	O(5)-Cd(2)-O(2)	89.23(19)	O(5)B-Cd(2)-O(2)B	89.23(19)
O(5)-Cd(2)-O(4)B	79.70(18)	O(2)-Cd(2)-O(4)B	97.62(18)	O(5)-Cd(2)-O(4)	100.30(18)
O(2)-Cd(2)-O(4)	82.38(18)	O(2)B-Cd(2)-O(4)	97.62(18)	Cd(2)-O(2)-Cd(1)	93.46(17)
Cd(1)A-O(3)-Cd(1)	100.27(18)	Cd(2)-O(4)-Cd(1)	90.71(16)		

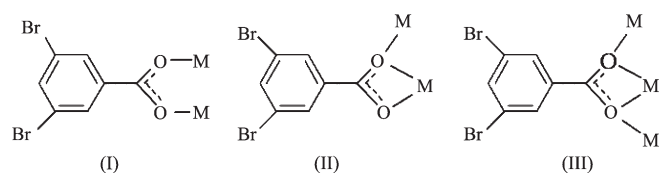| 2					
Mn(1)-O(1)	0.219 2(5)	Mn(1)-O(2)	0.243 8(5)	Mn(1)-O(4)A	0.207 4(5)
Mn(1)-O(5)A	0.242 4(5)	Mn(1)-O(6)A	0.240 1(5)	Mn(1)-O(6)B	0.215 7(4)
Mn(1)-N(1)	0.224 9(7)	Mn(2)-O(2)	0.215 0(5)	Mn(2)-O(2)A	0.215 0(5)
Mn(2)-O(3)	0.212 8(5)	Mn(2)-O(3)A	0.212 8(5)	Mn(2)-O(5)	0.226 3(4)
Mn(2)-O(5)A	0.226 3(4)				
O(4)A-Mn(1)-O(6)B	88.64(19)	O(4)A-Mn(1)-O(1)	91.2(2)	O(6)B-Mn(1)-O(1)	98.24(18)
O(4)A-Mn(1)-N(1)	172.1(2)	O(6)B-Mn(1)-N(1)	97.6(2)	O(1)-Mn(1)-N(1)	92.7(2)
O(4)A-Mn(1)-O(6)A	90.89(19)	O(6)B-Mn(1)-O(6)A	79.48(19)	O(1)-Mn(1)-O(6)A	176.85(18)
N(1)-Mn(1)-O(6)A	85.5(2)	O(4)A-Mn(1)-O(5)A	86.53(19)	O(6)B-Mn(1)-O(5)A	132.88(16)
O(1)-Mn(1)-O(5)A	128.68(17)	N(1)-Mn(1)-O(5)A	85.6(2)	O(6)A-Mn(1)-O(5)A	53.80(15)
O(4)A-Mn(1)-O(2)	91.55(18)	O(6)B-Mn(1)-O(2)	154.29(18)	O(1)-Mn(1)-O(2)	56.04(17)
N(1)-Mn(1)-O(2)	85.0(2)	O(6)A-Mn(1)-O(2)	126.22(17)	O(5)A-Mn(1)-O(2)	72.75(16)
O(3)-Mn(2)-O(2)A	89.3(2)	O(3)-Mn(2)-O(2)	90.7(2)	O(3)A-Mn(2)-O(5)	83.78(18)
O(3)-Mn(2)-O(5)	96.22(18)	O(2)A-Mn(2)-O(5)	81.55(18)	O(2)-Mn(2)-O(5)	98.45(18)
O(3)-Mn(2)-O(5)A	83.78(18)	Mn(2)-O(2)-Mn(1)	96.93(18)	Mn(2)-O(5)-Mn(1)A	94.36(17)
Mn(1)C-O(6)-Mn(1)A	100.52(19)				

Symmetry transformations used to generate equivalent atoms: A: −x, −y, −z+2; B: −x+1, −y, −z+2 for **1**; A: −x+1, −y+1, −z+1; B: x+1, y, z; C: x−1, y, z for **2**
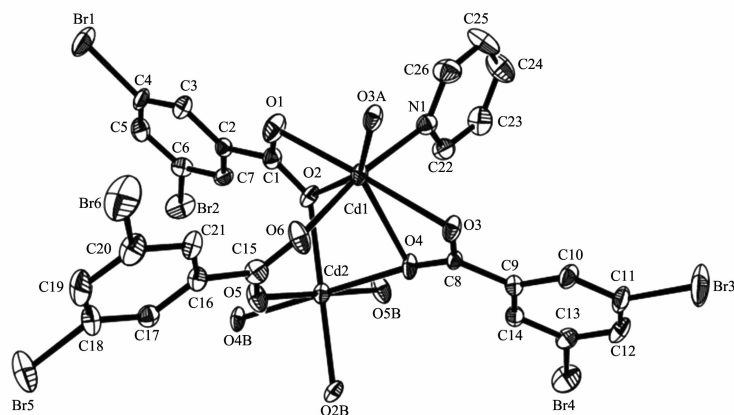
2　Results and discussion

2.1　Description of the structure

The X-ray crystallography analyses reveal that compounds **1** and **2** are isostructural; hence, only the structure of complex **1** is described in detail here. The asymmetric unit of compound **1** contains two crystallographically unique Cd(Ⅱ) atoms, three 3,5-Br$_2$BC$^-$ ligands, and one py moiety. As depicted in Fig.1, the Cd1 atom is seven-coordinated by six O atoms of four different 3,5-Br$_2$BC$^-$ ligands, and one N atom of py ligand, constructing a distorted pentagonal bipyramid. The Cd2 atom possesses a distorted octahedral coordination geometry, filled by six O atoms of six different 3,5-Br$_2$BC$^-$ ligands. The Cd-O (0.218 8(5)~0.250 5(5) nm) and Cd-N (0.229 5(6) nm) bond lengthes are in good agreement with those distances observed in some other Cd(Ⅱ) compounds[1,11-12]. In **1**, the 3,5-Br$_2$BC$^-$ ligands adopt three different coordination modes (Scheme 1), in which the carboxylate groups show the μ_2-η^1:η^1 bidentate, μ_2-η^1:η^2 tridentate, and μ_3-η^2:η^2 quadridentate modes. The carboxylate groups of 3,5-Br$_2$BC$^-$ ligands bridge alternately neighboring Cd(Ⅱ) ions to form a chain with the Cd⋯Cd separation of 0.347 54(6) and 0.366 00(8) nm (Fig.2). Adjacent chains are assembled to a 3D supramolecular framework through Br⋯Br (Br⋯Br: 0.334 7(4) nm) halogen bonding and C−H⋯Br
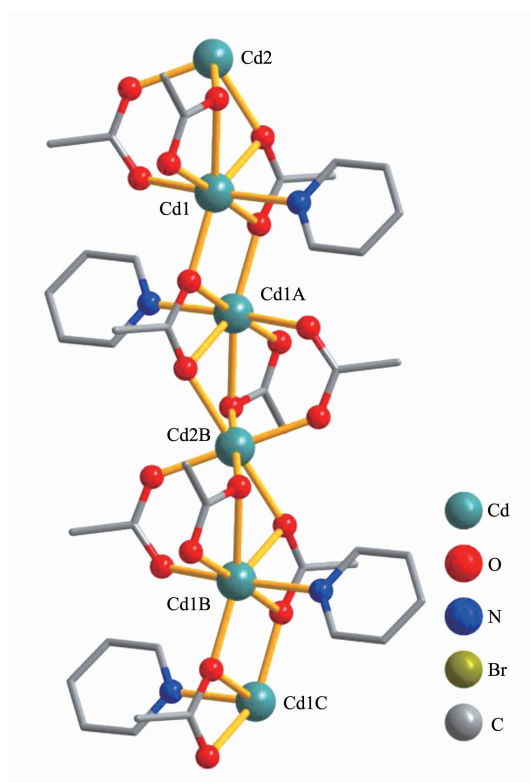
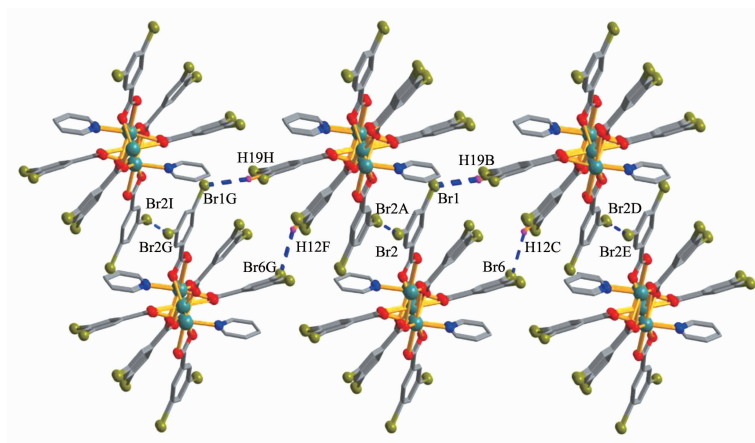Scheme 1　Coordination modes of 3,5-Br$_2$BC$^-$ ligands in compound **1**

H atoms were omitted for clarity; symmetry codes: A: $-x$, $-y$, $-z+2$; B: $-x+1$, $-y$, $-z+2$

Fig.1　Drawing of the asymmetric unit of compound **1** with thermal ellipsoids at 30% probability

The benzene rings of the 3,5-Br$_2$BC$^-$ ligands were omitted for clarity; Symmetry codes: A: $-x$, $-y$, $-z+2$; B: $x-1$, y, z; C: $-x-1$, $-y$, $-z+2$

Fig.2　A perspective of 1D chain of **1** along the ab plane

Dashed lines present the Br···Br interactions and the C-H···Br H-bond, symmetry codes: A: $-x+3$, $-y+1$, $-z+1$; B: $-x+2$, $-y+1$, $-z$; C: $x+2$, $y+1$, $z-2$; D: $-x+3$, $-y+1$, $-z$; E: $x+1$, y, $z-2$; F: x, $y+1$, $z-1$; G: $x+1$, y, z; H: $-x+2$, $-y+1$, $-z+1$; I: $-x+2$, $-y+1$, $-z+2$

Fig.3　A perspective of 3D supramolecular structure of **1** along the bc plane

hydrogen bond (Fig.3).

2.2　TGA analysis and PXRD results

To determine the thermal stability of compounds **1** and **2**, their thermal behaviors were investigated under nitrogen atmosphere by thermogravimetric analysis (TGA). As shown in Fig.4, the TGA curves of the compounds indicate that they are stable up to 142 ℃ and 150 ℃, respectively. Further heating leads to their decomposition. The powder X-ray diffraction experiments were carried out for compounds **1** and **2**. The patterns for the as-synthesized bulk material closely match the simulated ones from the single-crystal structure analysis, which is indicative of the pure solid-state phase (Fig.5 and Fig.6).

2.3　Luminescent properties

The emission spectra of 3,5-HBr$_2$BC and compound **1** were measured in the solid state at room
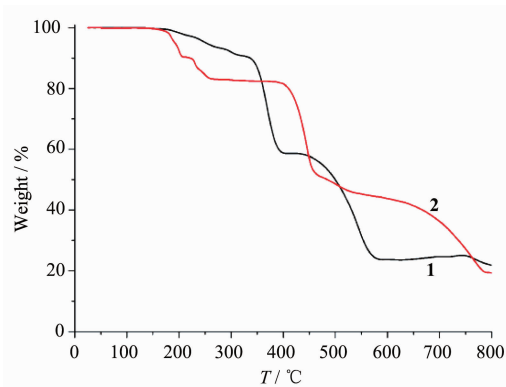

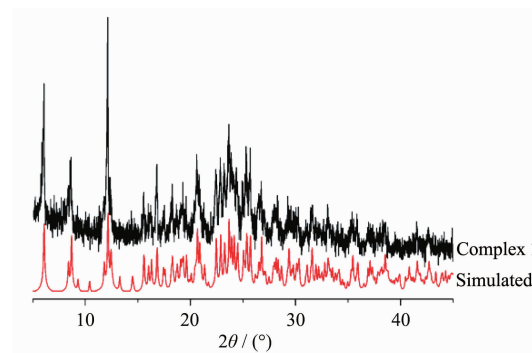Fig.4　TGA plots of compounds **1** and **2**

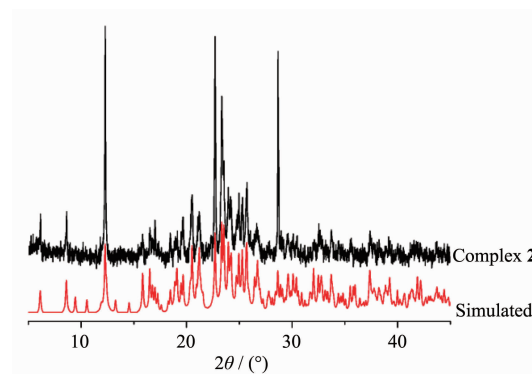Fig.5　PXRD pattern of compound **1** at room temperature

Fig.6　PXRD pattern of compound **2** at room temperature

temperature, as depicted in Fig.7. The "free" 3,5-HBr$_2$BC ligand displays a weak photoluminescence with an emission maximum at 480 nm if excited at 330 nm excitation. For the compound **1**, the significantly more intense emission band is observed with a maximum at 501 nm (λ_{ex}=330 nm), which can be assigned to the intraligand ($\pi^* \rightarrow n$ or $\pi^* \rightarrow \pi$)
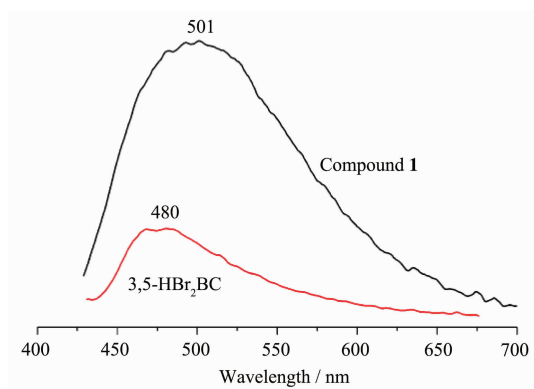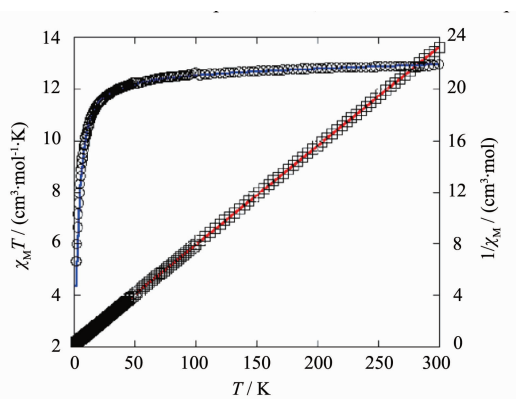
Fig.7 Solid state emission spectra of 3,5-HBr$_2$BC and compound **1**

emission [20]. The luminescence enhancement in compound **1** can be attributed to the binding of ligands to the metal centers, which effectively increases the rigidity of the ligand and reduces the loss of energy by radiationless decay[21].

The observed strong photoluminescence of **1** indicates that this compound can be an excellent candidate for potential application as a photoactive material.

2.4 Magnetic properties

The temperature-dependent magnetic properties of **2** are shown in Fig.8 in the form of $\chi_M T$ versus T curve. The $\chi_M T$ value of 12.94 cm$^3\cdot$mol$^{-1}\cdot$K at room temperature is close to that of 13.14 cm$^3\cdot$mol$^{-1}\cdot$K expected for the three magnetically isolated high-spin Mn(Ⅱ) ions (S_{Mn}=5/2, g=2.0). The $\chi_M T$ values steadily decrease with decreasing the temperature to reach the

The curve represents the best fit to the equations in the text; The line shows the Curie-Weiss fitting

Fig.8 Temperature dependence of $\chi_M T$ and $1/\chi_M$ vs. T for compound **2**

minimum values of 5.31 cm$^3\cdot$mol$^{-1}\cdot$K at 1.99 K. Between 1.99 and 300 K, the magnetic susceptibilities can be fitted to the Curie-Weiss law with C_M=13.30 cm$^3\cdot$mol$^{-1}\cdot$K and θ=−3.50 K. These results indicate an antiferromagnetic interaction between the nearest Mn(Ⅱ) ions.

We tried to fit the magnetic data of **2** using the following expression for a 1D Mn(Ⅱ) chain[22]:

$$\chi_{chain} = [Ng^2\beta^2/(kT)](A+Bx^2)(1+Cx+Dx^3)^{-1}$$

with A=2.925 4, B=209.87, C=16.497, D=2 738.6 and x=$J/(kT)$

Using this rough model, the susceptibilities for **2** were simulated, leading to J=−8.8 cm^{-1}, g=2.08, and the agreement factor R=4.63×10^{-6}.

References:

[1] Lu W G, Su C Y, Lu T B, et al. *J. Am. Chem. Soc.*, **2006**, **128**:34-35

[2] Kurmoo M. *Chem. Soc. Rev.*, **2009**,**38**:1353-1379

[3] Paul M, Adarsh N N, Dastidar P. *Cryst. Growth Des.*, **2014**, **14**:1331-1337

[4] Zhou J, Du L, Qiao Y F, et al. *Cryst. Growth Des.*, **2014**,**14**: 1175-1183

[5] Zheng X D, Lu T B. *CrystEngComm*, **2010**,**12**:324-336

[7] Ma L Q, Abney C, Lin W B. *Chem. Soc. Rev.*, **2009**,**38**: 1248-1256

[8] Li J R, Kuppler R J, Zhou H C. *Chem. Soc. Rev.*, **2009**,**38**: 1477-1504

[9] Fere G, Serre C. *Chem. Soc. Rev.*, **2009**,**38**:1380-1399

[10]Cui Y J, Yue Y F, Qian G D. *Chem. Rev.*, **2012**,**112**:1126-1162

[11]Gu J Z, Gao Z Q, Tang Y. *Cryst. Growth Des.*, **2012**,**12**: 3312-3323

[12]Gu J Z, Kirillov A M, Wu J, et al. *CrystEngComm*, **2013**,**15**: 10287-10303

[13]Zhang Y, Guo B B, Li L, er al. *Cryst. Growth Des.*, **2013**,**13**: 367-376

[14]Dong M M, He L L, Fan Y J, et al. *Cryst. Growth Des.*, **2013**,**13**:3353-3364

[15]Zhang L L, Guo Y, Wei Y H, et al. *J. Mol. Struct.*, **2013**,**1038**:73-77

[16]ZHANG Lai-Jun(张来军), TONG Ji-Zao(童吉灶), CHEN Fa-Yun(陈发云), et al. *Chinese J. Inorg. Chem.*(无机化学学报), **2014**,**30**(3):550-556

[17]Zang S Q, Fan Y J, Li J B, et al. *Cryst. Growth Des.*, **2011**,

11:3395-3405

[18]Zang S Q, Dong M M, Fan Y J, et al. *Cryst. Growth Des.*, **2012**,**12**:1239-1246

[19]Sheldrick G M. *SHELXL NT Version* 5.1, *Program for Solution and Refinement of Crystal Structures*, University of Göttingen, Germany, **1997**.

[20]Sun D, Han L L, Yuan S, et al. *Cryst. Growth Des.*, **2013**,**13**,377-385

[21]Zhang Y, Guo B B, Li L, et al. *Cryst. Growth Des*., **2013**, **13**,367-376

[22]Hiller W, Strähle J, Datz A, et al. *J. Am. Chem. Soc.*, **1984**,**106**,329-335